Published in final edited form as:
Dev Cell. 2010 September 14; 19(3): 365–376. doi:10.1016/j.devcel.2010.08.008.

A Zyxin-Mediated Mechanism for Actin Stress Fiber Maintenance and Repair

Mark A. Smith[1], **Elizabeth Blankman**[1], **Margaret L. Gardel**[2], **Laura Luettjohann**[1], **Clare M. Waterman**[3,*], and **Mary C. Beckerle**[1,*]

[1] Departments of Biology and Oncological Sciences, Huntsman Cancer Institute, University of Utah, Salt Lake City, Utah [2] Department of Physics, University of Chicago, Chicago, Illinois [3] Laboratory of Cell and Tissue Morphodynamics, Cell Biology and Physiology Center, National Heart, Lung and Blood Institute, National Institutes of Health, Bethesda, Maryland

Summary

To maintain mechanical homeostasis, cells must recognize and respond to changes in cytoskeletal integrity. By imaging live cells expressing fluorescently tagged cytoskeletal proteins, we observed that actin stress fibers undergo local, acute, force-induced elongation and thinning events that compromise their stress transmission function, followed by stress fiber repair that restores this capability. The LIM protein, zyxin, rapidly accumulates at sites of strain-induced stress fiber damage and is essential for stress fiber repair and generation of traction force. Zyxin promotes recruitment of the actin regulatory proteins, α-actinin and VASP, to compromised stress fiber zones. α-Actinin plays a critical role in restoration of actin integrity at sites of local stress fiber damage, while both α-actinin and VASP independently contribute to limiting stress fiber elongation at strain sites, thus promoting stabilization of the stress fiber. Our findings demonstrate a mechanism for rapid repair and maintenance of the structural integrity of the actin cytoskeleton.

Introduction

Organized tissues respond adaptively to mechanical changes in their environment. For example, muscle tissue undergoes a hypertrophic response to increased mechanical load, and an atrophic response to lack of load (Sadoshima and Izumo, 1997). Although much less well understood, non-muscle cells are also acutely sensitive to mechanical changes in their surroundings. The ability to sense and respond to changes in mechanical input is essential for many developmental processes (Wozniak and Chen, 2009) including tissue morphogenesis (Hutson et al., 2003), proliferation (Iwamoto et al., 2000; Peyton et al., 2006) and differentiation (Farge, 2003). Experimental disruption of intracellular force generation impedes a range of functions, including directed migration (Lo et al., 2004), cell sorting in tissues (Krieg et al., 2008), and stem cell lineage commitment (McBeath et al., 2004). Moreover, misregulation of the ability to sense and respond to mechanical cues is involved in many disease processes including pathological cardiac hypertrophy (Heydemann and McNally, 2007; Palmer, 2005) and tumor metastasis (Clark et al., 2000; Paszek and

[*]Corresponding authors: [1]Huntsman Cancer Institute, University of Utah, Salt Lake City, UT 84112, T: 801-581-4485, F: 801-581-2175, mary.beckerle@hci.utah.edu. [3] Cell Biology and Physiology Center, National Heart, Lung and Blood Institute, National Institutes of Health, Bethesda, MD, 20892, T:301-435-2949,F: 301-480-6012, watermancm@nhlbi.nih.gov.

Weaver, 2004). Consequently, understanding how cells sense mechanical cues within a physically diverse environment and respond by balancing forces and mechanical properties has emerged as a key to understanding how tissue homeostasis is maintained.

The actomyosin cytoskeleton is the major mediator of cellular mechanical properties. Actin filaments in non-muscle cells form linear contractile bundles of filaments called stress fibers (SFs) that are induced to assemble by activation of Rho, which promotes myosin-dependent contractility (Chrzanowska-Wodnicka and Burridge, 1996). SFs are common in cells cultured *in vitro* and are also found *in vivo* where they are induced to assemble when cells are exposed to mechanical stress, as in the vasculature (Byers et al., 1984). SFs possess a periodic distribution of α-actinin and myosin II, reminiscent of, although less organized than, the sarcomeric banding pattern in muscle (Langanger et al., 1986; Lazarides and Burridge, 1975). SFs terminate at extracellular attachment sites, such as focal adhesions (FAs), where they are linked via a network of proteins to integrins, transmembrane receptors that bind extracellular matrix (ECM) (Burridge et al., 1988). This transmembrane linkage enables bi-directional communication of mechanical information for sensing, generating, and responding to physical cues. For example, actomyosin-dependent contractile forces generated by SFs are transmitted to the extracellular environment (Harris et al., 1980; Lauffenburger and Horwitz, 1996; Wang et al., 1993), a process critical for cell motility, extracellular matrix remodeling, and tissue morphogenesis. Reciprocally, externally applied strains and stresses promote SF thickening and reorientation (Iba and Sumpio, 1991; Yoshigi et al., 2005). Although it is well established that the actomyosin cytoskeleton is essential for physical cell behavior and mechanosensing, and responds dynamically to a variety of biochemical signals, little is known about the molecular mechanism by which SFs sense or respond to mechanical perturbations.

The LIM protein, zyxin, is responsive to mechanical cues. Zyxin localizes to SFs and is required for SF thickening in response to cyclic cell stretch (Yoshigi et al., 2005). The K_{off} of FA-localized zyxin is increased when the associated SF is severed by laser surgery (Lele et al., 2006). Retrograde fluxes of zyxin at FAs are abated in response to decreased myosin contractility and increase in response to applied force (Guo and Wang, 2007). Finally, zyxin has been shown to be recruited to substrate anchor points on laser severed SFs (Colombelli et al., 2009), and to reversibly accumulate on SFs and FAs in response to mechanical perturbation (Colombelli et al., 2009). However, little is known about what role zyxin's mechanical responsiveness plays in cells in the absence of externally applied stress. Furthermore, the mechanism by which zyxin drives functional adaptation and remodeling of the actin cytoskeleton remains uncharacterized.

Here we have dissected a molecular mechanism by which actin SFs in non-muscle cells maintain their integrity in response to acute mechanical failure. We observed that SFs undergo local, acute, stress-induced elongation and thinning events. Some of these events are repaired, while others progress to catastrophic breaks. These strain events are triggered by stress increases in the SF and they compromise SF force transmission function. Zyxin and its partners accumulate at SF strain sites and facilitate their repair. In cells lacking zyxin the strain site repair capacity is compromised, and as a result of the diminished structural integrity of SFs, whole cell force transmission is attenuated. Our findings demonstrate a SF-resident system for rapid repair and maintenance of the actin cytoskeleton.

Results

Actin Stress Fibers Exhibit Acute, Local Thinning and Elongation Leading to Either Catastrophic Breakage or Repair

To understand how SFs in living cells maintain their physical integrity, we performed time-lapse imaging of mouse fibroblasts expressing actin-mCherry and looked for evidence of SF remodeling. This revealed spontaneous catastrophic breakage of SFs that occurred at a frequency of 0.03 +/−0.01 breaks/minute/cell (n=83 cells, 1100 minutes of observation). Prior to a break, SFs displayed elongation and thinning within a localized region that subsequently became the breakage site. The elongation/thinning phase persisted for 10–60 seconds. Immediately following development of a distinct discontinuity, the flanking regions of the SF underwent rapid retraction, and we observed a persistent loss of actin fluorescence along the previous path of the SF indicating catastrophic breakage (Figure. 1, A–C and Movie S1), reminiscent of myosin II-dependent SF elastic recoil after laser severing (Kumar et al., 2006).

We also noted that for many sites of acute, local SF elongation and thinning, instead of progressing to a catastrophic break, the strain site exhibited spontaneous restoration of actin integrity (Figure 1 D–F and Movie S1) providing the first indication of a mechanism for SF repair. We refer to this actin remodeling as SF repair, since, as is described below, when the remodeling machinery is compromised, the incidence of SF breaks increases. Local, acute SF thinning, elongation and restoration events arose spontaneously at a rate of 0.18 +/− 0.03 events/minute/cell (n=83 cells, 1100 minutes of observation). Quantitative features of these events are summarized in Supplementary Table 1. Following SF thinning, the mean recovery rate of actin fluorescence signal within the strain site was 1.20 +/− 0.18 fluorescence intensity units/second (n=10), resulting in recovery to 142.6 +/− 12% (n=11) of the original actin fluorescence signal during a 500 second analysis period. Kymograph analysis of fiducial marks flanking the strain site showed that the average maximum elongation distance was 2.5 +/− 0.2μm (n=10), nearly twice the inter-sarcomeric SF banding distance which ranges from 0.4–1.75μm (our observation and (Peterson et al., 2004)). Local SF elongation occurred at a rate of 4.0 +/− 1.4 μm/min; (n=10). The half-time to cessation of elongation was 77 +/− 6 seconds (n=10). Actin fluorescence signal recovery typically occurred at a uniform rate across the strain site and was not accompanied by rejoining of the separated fiducial marks. This suggests that restoration occurred primarily by addition of new actin along the length of the residual thinned SF, as opposed to reversal of the elongation phase. Of SFs that experienced an acute, local elongation event, 82% recovered, while 18% progressed to a catastrophic break. These events are distinct from previously described internal SF elongations (Peterson et al., 2004), with 5–10 fold greater elongation length and >100 fold higher elongation velocities. Thus, our findings demonstrate that SFs undergo spontaneous, acute, local strain events that may or may not repair, providing evidence for a mechanism by which the majority of damaged SFs are repaired *in situ*.

Zyxin is Recruited to Sites of Stress Fiber Strain

How are acute, local SF strain events detected, stabilized and restored? Previous findings showing that the LIM protein zyxin responds to mechanical stress (Hoffman et al., 2006; Yoshigi et al., 2005) led us to consider a role for zyxin in repair of acute, local SF strain. Consistent with this hypothesis, in cells expressing zyxin-GFP and actin-mCherry we observed that in addition to normal localization at FAs and periodic punctae along SFs, zyxin rapidly and robustly accumulated at sites of acute, local SF strain (Figure 2, A–C and Movies S2 and S3). Analysis of kymographs (Figure 2B) revealed that local SF strain immediately preceded zyxin accumulation, which in turn preceded restoration of actin at the strain site (Figure 2C). The average t½ for zyxin accumulation at SF strain sites was 28.6 +/

− 3.7 seconds (n=24). From its maximum intensity, zyxin associated with the strain site displayed a half-life of 112 +/− 12 seconds (n=10), leaving the SF more slowly than it accumulated. The dissociation rate of zyxin from sites of acute SF damage is an order of magnitude slower than the dissociation rate of zyxin we measured by FRAP from stable SF regions (t1/2 = 13 +/− 1.5 seconds (n=61)) (Figure S1A-C). Thus, acute, local SF strain elicits rapid zyxin recruitment through a novel mode of zyxin/SF interaction.

Mechanical Stimulation Triggers Local Accumulation of Zyxin at Sites of Stress Fiber Strain

The accumulation of zyxin that we observed at sites of acute SF strain, coupled with the finding that zyxin exhibits force-sensitive binding to cellular structures (Lele et al., 2006; Yoshigi et al., 2005) led us to hypothesize that acute, local zyxin accumulation on a SF could be induced by physical perturbation. To test this, we grew zyxin-GFP expressing cells on fibronectin-coupled elastic polyacrylamide substrates (Beningo et al., 2002), then prodded the cell cortex with a polished micropipette (Fig 2D and Movie S4). At the site of cortical deformation, we observed SF deflection and concomitant rapid, local accumulation of zyxin-GFP on the SF. This finding supports the hypothesis that direct application of mechanical force is sufficient to initiate rapid zyxin accumulation to regions of local SF strain.

Stress Fiber Strain Events Do Not Generate New Focal Adhesions

It is possible that the rapid accumulation of zyxin to sites of acute SF strain could represent the formation of new FAs. Formation of a FA would be indicated by accumulation of the FA protein vinculin (Zamir and Geiger, 2001) and local induction of stress transmission to the substrate (Beningo et al., 2002; Gardel et al., 2008). Observation of cells co-expressing zyxin-GFP and vinculin-mCherry revealed lack of coordinate vinculin accumulation with zyxin at sites of SF strain (Figure 2E and F). To determine if local zyxin accumulation at SF strain sites was correlated with stress transmission to the substrate, we plated cells expressing zyxin-GFP on fiducial-embedded polyacrylamide substrates and performed high-resolution traction-force microscopy (Sabass et al., 2008). Although we detected extensive substrate strain at FAs, changes in traction force were not observed at zyxin-rich SF strain sites (Fig 2G and Movie S5). Many sites of rapid zyxin accumulation underwent lateral movement that was coordinated with movement of the SF, providing further evidence that these sites were not substrate-bound. These data show that local, rapid zyxin accumulation at strain sites is not associated with formation of new FAs, but rather represents targeted accumulation of zyxin on a SF.

Stress Fiber Strain Events are Preceded by Elevated Contractility and Reduce Traction Force

What induces SF strain events in steady state cells, and what is the mechanical output of these events? Since mechanical perturbation is sufficient to induce strain events, we wanted to test whether SFs exerted increased contractile force prior to the strain event. To test this, we used traction force microscopy to simultaneously measure local zyxin-GFP accumulation on a SF and relative substrate traction at the FA where the associated SF terminates (Fig 2G-I and Movie S5). We compared local substrate traction forces at FAs during periods of quiescence and during acute, local SF elongation accompanied by rapid accumulation of zyxin. During quiescent periods, substrate traction force was relatively stable during a 30 second measurement interval (Figure 2H). In contrast, immediately prior to periods of rapid SF elongation and zyxin accumulation, substrate traction force at the site of associated FAs increased by an average of 15% (Figure 2H). This indicates that increasing SF contractility precedes the development of SF strain events.

We reasoned that acute, local SF strain may reduce the transmission of force through the cytoskeleton to the ECM. A zyxin-mediated repair process could restore this capacity. Immediately after periods of rapid SF elongation and zyxin accumulation, substrate traction force at the site of associated FAs decreased by an average of 40% (Figure 2H). Kinetic analysis showed that as SF strain site length stabilized and zyxin intensity plateaued, substrate traction forces at the FA were restored (Figure 2I). We conclude that SFs undergo acute, local strain, in response to escalating stress, causing a reduction in their ability to transmit force through their associated FA to the ECM. Recruitment of zyxin to SF strain sites accompanies restoration of the cell's capacity to exert traction on the substrate.

Zyxin Null Cells Exhibit Impaired Stress Fiber Repair and Increased Stress Fiber Breakage

To determine the requirement for zyxin in the SF repair process, we characterized the SF break frequency and the recovery of actin at acute, local SF strain sites in fibroblasts derived from zyxin (−/ −) mice (Hoffman et al., 2006). We found that zyxin (−/ −) cells displayed a profound deficiency in their ability to restore actin levels at acute SF strain sites (Figure 3A and B and Movie S6), and exhibited a greater than five-fold increase in the frequency of catastrophic SF breaks when compared to wild-type cells (Figure 3C). To confirm the increased SF breakage was directly due to the absence of zyxin, we expressed full-length zyxin-GFP in zyxin (−/ −) cells and restored wild-type behavior (Figure 3C and S1D). Consistent with the increase in catastrophic SF breaks, zyxin (−/ −) cells exhibited a significant drop in the rate and percent of actin-mCherry fluorescence recovery at the strain site when compared to zyxin (−/ −) cells expressing zyxin-GFP (Figure 3D and E). In addition, the half-time to cessation of elongation and the extent of SF strain were two to three-fold higher in cells lacking zyxin, as compared to zyxin (−/ −) cells expressing zyxin-GFP (Figure 3F and G). These data demonstrate that zyxin is critical for maintaining SF integrity by detecting damage and mediating rapid SF repair.

Zyxin Null Cells Exhibit Decreased Force Generation Capacity

We postulated that zyxin's contribution to SF maintenance would be critical for the SF's ability to generate and transmit force to the substrate. By comparing whole cell traction forces in zyxin (−/ −) cells, with and without zyxin-GFP rescue, we found that peak forces transmitted to the substrate were significantly decreased in cells lacking zyxin (Figure 3H and S2). Collagen plug contraction assays (Grinnell, 2000) confirmed that zyxin (−/ −) cells display compromised capacity to exert force on the extracellular matrix (Figure 3I). Since substrate adhesion is not diminished in zyxin (−/ −) cells (Hoffman et al., 2006), zyxin's impact on force generation capacity could be due to a role in maintaining actin cytoskeletal integrity, influence on actomyosin-dependent contractility, or both. The diminished SF repair and enhanced SF break frequency observed in zyxin (−/ −) cells supports the view that zyxin contributes directly to maintenance of cytoskeletal integrity. We detected no zyxin-dependent difference in global myosin light chain phosphorylation (Figure 3J), a surrogate marker for actomyosin-dependent contractility.

Stress Fiber Strain Sites are Rich in Free Barbed Actin Filament Ends and Accumulate α-Actinin and VASP in a Zyxin-Dependent Manner

How does zyxin accumulation mediate restoration of actin and SF integrity in response to an acute SF strain event? The rapid restoration of SF integrity at SF strain sites raised the possibility that the strain site was rich in uncapped actin filament barbed ends that could be extended by actin polymerization. To test this hypothesis, we performed actin barbed end assays on live cells experiencing strain events. We observed that rhodamine-labeled G-actin was rapidly recruited at SF strain sites (Figure 4A and Movie S7) indicating the presence of actin barbed ends at these sites and displaying a striking correspondence with the zyxin-rich region.

Zyxin interacts directly with the F-actin cross-linking protein α-actinin (Crawford et al., 1992; Reinhard et al., 1999), as well as with the actin polymerization regulator, and actin barbed end binding protein VASP (Drees et al., 2000; Niebuhr et al., 1997). To determine whether α-actinin and/or VASP cooperate with zyxin in the SF restoration response, we examined their dynamic behaviors during acute SF strain and restoration using time-lapse imaging of fluorescently tagged zyxin and α-actinin or VASP.

α-Actinin was recruited to sites of acute SF strain with kinetics that lagged zyxin accumulation (Figure 4B–D and Movie S8). To test whether α-actinin is dependent on zyxin for accumulation at SF strain zones, we examined the ability of α-actinin to accumulate on SFs in zyxin (−/ −) cells. In the absence of zyxin, α-actinin displayed a typical periodic distribution on SFs (Figure 4E), illustrating that zyxin is not essential for targeting α-actinin to these structures. However, rapid accumulation of α-actinin at zones of acute SF strain that did not immediately progress to breakage was profoundly compromised in cells lacking zyxin and was restored in cells re-expressing zyxin-GFP (Figure 4F and Movie S8), demonstrating that zyxin is required, either directly or indirectly, for specific localized α-actinin recruitment to sites of acute SF strain.

In zyxin (−/ −) cells reconstituted with zyxin-mCherry, VASP-GFP was recruited to SF strain sites with kinetics similar to that of zyxin (Fig 4D, G, H, and Movie S9) and localized to both SFs and FAs. Consistent with previous reports (Hoffman et al., 2006), VASP localization to FAs and SFs was compromised in zyxin (−/ −) cells (Figure 4I). VASP recruitment to acute SF strain sites that did not immediately progress to breakage was also abolished in zyxin (−/ −) cells, and restored by re-expression of zyxin-mCherry (Figure 4J and Movie S9). In pair-wise comparison of the recruitment half-times, we observed that α-actinin lagged VASP by an average of 34 seconds (n=9, $P<0.05$)(Figure 4K). Together, these results indicate a requirement for zyxin in recruitment of the actin regulatory proteins α-actinin and VASP to sites of SF strain, and define a temporal ordering of recruitment with VASP and zyxin co-recruited, followed by α-actinin.

Zyxin Recruitment to Acute Stress Fiber Strain Sites is Not Dependent on Interactions with α-Actinin or VASP

To determine whether zyxin accumulation at SF strain sites depends on its ability to interact directly with either α-actinin or VASP, we generated GFP-tagged zyxins bearing mutations that disrupt interaction with either α-actinin or Ena/VASP family members, co-expressed them with actin-mApple in zyxin (−/ −) cells, and imaged acute SF strain sites. To disrupt α-actinin binding to zyxin, we deleted the first 42 amino acids of zyxin to make zyxΔ1-42-GFP (Nix et al., 2001; Reinhard et al., 1999) (Figure 5A). To disrupt zyxin binding to Ena/VASP family members, we mutated the phenylalanines to alanine in each of zyxin's four proline-rich (FPPP) sequences (ActA repeats) to make zyx4F>A-GFP (Drees et al., 2000) (Figure 5A). Neither the FA nor SF localization of zyxin was perturbed by mutation of zyxin's α-actinin or Ena/VASP binding sites (Figure 5B). Moreover, rapid recruitment to acute SF strain sites occurred for both zyxΔ1-42-GFP (Figure 5C and D) and zyx4F>A-GFP (Figure 5E and F). Kinetic analysis revealed that zyxΔ1-42 recruitment was indistinguishable from recruitment of zyxin-GFP, however zyx4F>A recruitment was slower (Figure 5G). These data suggest that zyxin does not depend on association with either α-actinin or Ena/VASP for localization to sites of acute SF strain. However, the rate of zyxin recruitment to SF strain sites may be increased through interaction with VASP.

α-Actinin and VASP Require Interaction with Zyxin for Recruitment to Acute Stress Fiber Strain Sites

To determine whether zyxin binding is required for localization of α-actinin or VASP to acute SF strain sites, we examined the subcellular localization of α-actinin-mCherry or VASP-mCherry in zyxin (−/ −) cells re-expressing zyxΔ1-42-GFP or zyx4F>A-GFP to eliminate α-actinin or Ena/VASP binding, respectively. In zyxin (−/ −) cells expressing zyxΔ1-42-GFP, α-actinin-mCherry localized to FAs and SFs (Figure 6A). However, α-actinin-mCherry failed to accumulate at sites of acute SF strain (Figure 6B–D)(Compare Figure 6B and C to Figure 4B and C). In zyxin (−/ −) cells expressing zyx4F>A-GFP, VASP-mCherry did not localize to SFs or FAs (Figure 6E). VASP-mCherry recruitment to sites of acute SF strain was also greatly attenuated (Figure 6F–H)(Compare Figure 6F and G with Figure 4G and H). Our results illustrate that compromising zyxin's ability to bind either α-actinin or VASP limits the capacity of these proteins to accumulate with zyxin at sites of local, acute SF strain, supporting the view that direct binding to zyxin contributes substantially to both α-actinin and VASP recruitment to SF strain sites.

α-Actinin and VASP have Distinct Roles in the Stabilization of SF Strain Sites

Both α-actinin and VASP modulate actin organization and dynamics. Therefore, we tested whether the zyxin-dependent repair of acute SF strain sites required α-actinin or VASP recruitment to these sites. We examined SF strain and repair events by imaging actin-mCherry in both zyxin (−/ −) cells expressing zyxin variants with compromised α-actinin or VASP binding functions. Quantification of actin-mCherry fluorescence at acute SF strain sites showed that expression of either zyxin-GFP or zyx4F>A-GFP in zyxin (−/ −) cells restored both the rate and extent of actin recovery at strain sites to wild-type levels (Figures 7A and B). In contrast, actin recovery at SF strain sites was reduced in zyxin (−/ −) cells whether or not they additionally expressed zyxΔ1-42-GFP (Figures 7A and B). Quantification of the time and distance of acute SF extension revealed that re-expression of wild-type zyxin-GFP in zyxin (−/ −) cells was sufficient to reduce the extent of SF strain to wild-type levels, while SF strain was increased in zyxin (−/ −) cells, whether or not they additionally expressed either zyxΔ1-42-GFP or zyx4F>A-GFP (Figure 7C and D). Thus, both α-actinin and VASP contribute to zyxin's ability to arrest acute, localized SF strain.

To determine how these proteins contribute to maintaining the overall integrity of actin SFs, we analyzed SF breakage frequency. This revealed that zyxin (−/ −) cells had an increased frequency of SF breakage compared to wild-type cells, whether or not they were expressing zyxΔ1-42-GFP. In contrast, expression of either zyxin-GFP or zyx4F>A-GFP in zyxin (−/ −) cells reduced the SF breakage frequency to wild-type levels (Figure 7E). Taken together, these results indicate that VASP and α-actinin have both common and distinct roles in assisting zyxin in SF repair at acute strain sites. Both α-actinin and VASP are required to stabilize elongation of local SF strain, while α-actinin has a primary role in restoring actin at the SF damage site and preventing strain events from progressing to catastrophic breaks.

Discussion

By observing the dynamics of SFs in living cells, we identified novel acute, local SF damage events that occur spontaneously in response to increasing intrinsic stress within the fibers, or in response to mechanical perturbation, and defined a molecular mechanism for rapid SF repair and homeostasis of the actin cytoskeleton. SFs that exhibit acute, local strain events display a transient reduction of force transmitted though associated FAs. Zyxin rapidly accumulates at acute SF strain sites where free barbed ends of actin filaments are concentrated, and zyxin facilitates the recruitment of binding partners, VASP and α-actinin, which together comprise a repair complex that effects repair and mechanical stabilization of

the SF. In the absence of zyxin, the incidence of catastrophic SF breaks is dramatically increased, and the capacity of the associated FAs to transmit forces to the substrate and retract a surrounding collagen gel is compromised (Figure 7F). The SF repair process restores the capacity of the SF to develop tension and convey traction forces to the ECM. Thus, SF strain events rapidly relieve cytoskeletal prestress, while simultaneously providing a clear target for a system that rebuilds the weakest region of the fiber, thereby enabling the cytoskeleton to tolerate dynamic increases in force load by sensing and repairing SF damage prior to failure. Without this repair system, cells exhibit a marked reduction in their ability to transmit force to remodel ECM, a process critical to tissue morphogenesis, maintenance and repair.

Both the direct application of mechanical stimulation or conditions of elevated internal SF contractility are sufficient to induce SF strain events. The zyxin-mediated repair complex is recruited within several seconds of the local strain event, suggesting a model in which new zyxin binding sites are generated at the SF strain site. Both FRAP and photoactivation of fluorescent zyxin (data not shown) indicate that zyxin on strain sites is rapidly exchanging with a cytoplasmic pool. However, how binding sites are created is not clear. While it has been proposed previously that a conformational change in α-actinin could be responsible for stress-induced recruitment of zyxin to SFs (Colombelli et al., 2009), our data indicate that zyxin accumulation at strain sites is independent of α-actinin binding and precedes α-actinin accumulation by tens of seconds. Alternatively, it is possible that local actin filament breakage and the resultant generation of free filament barbed ends which are concentrated at SF strain sites triggers recruitment of zyxin. Indeed, zyxin is present at FAs where actin filament barbed ends are concentrated and has been shown to accumulate at sites of laser-induced SF severing (Colombelli et al., 2009). Although a direct zyxin-actin interaction has not been reported, zyxin could be recruited to free barbed ends at strain sites as a co-complex with a barbed-end capping protein. Alternatively, strain-induced changes in the actin polymer or an associated protein other than α-actinin could reveal a new docking site for zyxin on the SF. Mechanical stimulation can reveal new epitopes on cytoskeleton-associated proteins, including talin (Lee et al., 2007) and p130Cas (Sawada et al., 2006). Zyxin accumulation could also be regulated by mechanically-induced local activation of kinases (Tamada et al., 2004; Wang et al., 2005), as is the movement of zyxin from FAs onto associated SF termini (Guo and Wang, 2007).

Independent of the mechanism of zyxin recruitment, our data indicate that both α-actinin and VASP participate in stabilizing elongation of acute SF strain sites. The presence of actin barbed ends throughout the SF strain site suggests that SF repair is at least in part the result of actin polymerization. Indeed, zyxin and VASP have been shown to facilitate actin polymerization (Barzik et al., 2005; Fradelizi et al., 2001; Hirata et al., 2008). However, within the sensitivity of our detection and analysis system, we did not observe a role for VASP in the restoration of actin at SF strain sites. Rather, VASP appeared to be coordinately recruited with zyxin to SF strain sites where it served to enhance the rate of zyxin accumulation, perhaps stabilizing a conformation that is compatible with its recruitment. The ability of α-actinin to crosslink actin filaments suggests that recruitment and bundling of preexisting actin polymer from the cytoplasm may restore actin density of the SF structure to restore mechanical integrity.

Cells that lack zyxin have enhanced migration relative to their wild-type counterparts (Hoffman et al., 2006), however the reason for this altered behavior was not understood. The loss of zyxin's contribution to the maintenance and structural stability of SFs in the knockout cells may contribute to this phenotype. In particular, it has long been appreciated that stationary cells are characterized by the presence of robust SFs whereas migratory cells display a much less robust complement of SFs. The increased migration velocity of zyxin

(−/ −) cells may be attributable, at least in part, to the reduced stability and integrity of actin SFs in the null cells, a condition that would be expected to support enhanced migratory capacity.

Homeostasis is a central concept in animal physiology that describes the ability of living organisms to maintain constancy of their internal environment. Prior work extended this paradigm to the subcellular level, where it is evident in the maintenance of organelles such as the endoplasmic reticulum (Cox et al., 1993; Kozutsumi et al., 1988) and to macromolecular complexes such as the genetic material (Branzei and Foiani, 2008). The novel mechanism of strain recognition and repair presented here demonstrates a cellular machinery for rapid adjustment of cytoskeletal tension in response to changes in cell contractility or extrinsic forces. The demonstration that SFs display an intrinsic capacity for self-monitoring and repair in response to mechanical stress further extends the concept of homeostasis to the cytoskeleton for the regulation of both cytoarchitecture and mechanical output.

Experimental Procedures

Materials

Cell lines—Production and immortalization of fibroblasts derived from wild-type and zyxin-null mice was described previously (Hoffman et al., 2006). Fibroblasts derived from zyxin (−/ −) mice were stably rescued with N-terminally tagged zyxin or mutant zyxin by viral infection followed by FACS sorting to select cells expressing fluorescently tagged zyxin (Hoffman et al., 2006).

Cell culture and transfection—Cells were cultured in DMEM supplemented with L-glutamine, penicillin/streptomycin, sodium pyruvate and 10% fetal bovine serum (Hyclone) and grown on coverslips coated with fibronectin (10 μg/ml.) Transient transfections of DNA constructs for expression of fluorescently tagged proteins were performed using FuGENE HD transfection reagent (Roche). Time lapse imaging of cells was performed 3–6 days after transfection.

DNA constructs—Constructs used are described in Supplemental Methods.

Analysis of myosin posphorylation

Cell lysates were harvested using SDS sample buffer and run on SDS-PAGE. Blots were probed with anti-phospho myosin light chain (ser19) (Cell Signaling Technology) then stripped and re-probed with anti-myosin light chain (Cell Signaling Technology) to control for total myosin light chain. Three independent experiments were conducted.

Collagen gel contraction assay

Collagen I gels made with 0.5×10^5 either zyxin (−/ −) cells or zyxin (−/ −) +zyxin-GFP were grown in 1.5mg/ml in 6mm diameter glass bottom wells. The gels released from the plastic edges of the wells on day 2, and were imaged on day 7. The final gel area was determined using ImageJ.

Live-cell imaging for protein dynamic studies

Coverslips were mounted in a closed chamber (LIS), with DMEM/F12 media (Invitrogen) supplemented with 10% fetal bovine serum. Cells were maintained at 37° C using a microscope temperature control system (LIS). Imaging was performed on an Andor spinning disk confocal on an inverted Nikon TE300 microscope with a 60X 1.4NA Nikon Plan

Apochromat lens. Illumination was from solid state 488nm and 568nm lasers (Melles Griot), switched by an acousto-optic tunable filter based laser combiner (Andor Technology), and delivered by optical fiber to the Yokogawa CSU-10 scanhead. The emission light path was equipped with a dual bandpass filter (Semrock Inc). All time-lapse image sequences were captured at 10 second intervals using either Andor DV887 1024X1024 EMCCD camera, or Andor DV885 512X512 EMCCD camera (Andor Technology). Stage motions were controlled in XY with a Ludl XY stage (Ludl Electronic Products) and in Z with a Piezo stage insert (Mad City Labs). Image acquisition was performed using Andor IQ imaging software (Andor Technologies) on a PC workstation (Dell Computers).

Live barbed ends assay—Cells were plated on poly-L-lysine coated coverslips, then were imaged at a 2second frame rate until a strain event was observed. The imaging chamber was quickly perfused with saponin/rhodamine-actin solution to permeablize and label actin barbed ends. Final labeling mixture formulation was .005% saponin, 0.5μM rhodamine-actin, 0.1mM ATP, 138nM KCl,10mM PIPES, 3mM EGTA, 4mM $MgCl_2$ (pH 6.9).

Direct manipulation of cells—Cells expressing zyxin-GFP for direct manipulation were plated on polyacrylamide substrates. They were prodded with a fire-polished glass pipette mounted on an Eppendorf micromanipulator. Images of this procedure were captured every 2 seconds using the imaging system described above.

Traction Microscopy

Methods used for traction microscopy are in Supplemental Methods

Image processing and analysis

Fluorescence intensity and SF elongation—Image sequences were processed, region intensity and distance measurements were collected, and movies were generated using MetaMorph software (Molecular Devices). Intensity measurements were taken as average intensity within a region of interest restricted to the site of SF elongation. Kymographs were generated using a custom macro (Ryan Littlefield) run in MetaMorph. For these, a 10 pixel wide linear region of interest along a SF was selected, the image was rotated using the nearest neighbors rotation algorithm to eliminate diagonal pixel sampling, and then each 10 pixel region was output into a montage. Distance measurements to assay SF elongation were made on the kymograph using two polylines overlaid on the kymograph flanking the site of SF extension. Each line followed a stable fluorescent intensity feature on the SF serving as a fiduciary mark. The distance change between the polylines was plotted over time. Numerical output was normalized and graphed using Prism 5 (GraphPad.)

Analysis of actin recovery—We tracked actin-mApple fluorescent average intensity within the strain region. Starting from the low point in the intensity plot, as the region entered the repair phase, we fit a line to the trajectory of recovery, restricted to the first 200 seconds of recovery, then calculated recovery rate (fluorescence intensity/time) based on the slope of this line. Percent actin signal recovery was calculated as the percent that actin signal within the thinning region recovered, relative to the original signal, within the 500 second imaging period.

Analysis of kinetics and elongation stabilization—For analysis of the kinetics of protein accumulation, intensity over time was fit using the Hill equation (Y=Vmax*X^h/(K^h + X^h). Analysis of dissipation was fit using the model for single phase exponential decay (Y=(Y0 − Plateau)*exp(−K*X) + Plateau). Half time to stabilization of elongation was determined using the Hill equation fit to elongation data.

Statistical analysis—All statistical analysis was performed using Prism 5 (GraphPad). Statistical significance for the analyses of SF breaks, changes in traction induced strain, the kinetics of fluorescence accumulation, and the kinetics of fluorescence dissipation were determined using unpaired, two-tailed t-tests. Contingency analyses of actin recovery and α-actinin and VASP recruitment utilized a two-tailed Fisher's exact test. Differences were considered significant at the 95% confidence level. Statistical significance denoted as follows; ***= $p<0.001$, **=$p=0.001$ to 0.01, *=$p=0.01$ to 0.05.

Supplementary Material

Refer to Web version on PubMed Central for supplementary material.

Acknowledgments

We thank Frank Gertler (Massachusetts Institute of Technology), Michael Davidson (Florida State University), Carol Otey (University of North Carolina, Chapel Hill) and Ke Hu (Indiana University) for reagents. We also thank Laura Hoffman and Chris Jensen for the zyx4F>A cell line, the zyx 1–42 construct and for helpful discussions, Jonathan Stricker for technical advice and Diana Lim for graphic design. Supported by NIH RO1GM50877 (M.C.B.), the Huntsman Cancer Foundation, and shared resources from the Cancer Center Support Grant (2 P30 CA042014-21), the NIH multidisciplinary cancer research training grant (M.A.S.), the Burroughs Wellcome Career Award at the Scientific Interfaces and NIH Director's Pioneer Award 5 DP1 OD003354-02 (M.L.G).

References

Barzik M, Kotova TI, Higgs HN, Hazelwood L, Hanein D, Gertler FB, Schafer DA. Ena/VASP proteins enhance actin polymerization in the presence of barbed end capping proteins. J Biol Chem. 2005; 280:28653–28662. [PubMed: 15939738]

Beningo KA, Lo CM, Wang YL. Flexible polyacrylamide substrata for the analysis of mechanical interactions at cell-substratum adhesions. Methods Cell Biol. 2002; 69:325–339. [PubMed: 12071003]

Branzei D, Foiani M. Regulation of DNA repair throughout the cell cycle. Nat Rev Mol Cell Biol. 2008; 9:297–308. [PubMed: 18285803]

Burridge K, Fath K, Kelly T, Nuckolls G, Turner C. Focal adhesions: transmembrane junctions between the extracellular matrix and the cytoskeleton. Annu Rev Cell Biol. 1988; 4:487–525. [PubMed: 3058164]

Byers HR, White GE, Fujiwara K. Organization and function of stress fibers in cells in vitro and in situ. A review. Cell Muscle Motil. 1984; 5:83–137. [PubMed: 6367964]

Chrzanowska-Wodnicka M, Burridge K. Rho-stimulated contractility drives the formation of stress fibers and focal adhesions. J Cell Biol. 1996; 133:1403–1415. [PubMed: 8682874]

Clark EA, Golub TR, Lander ES, Hynes RO. Genomic analysis of metastasis reveals an essential role for RhoC. Nature. 2000; 406:532–535. [PubMed: 10952316]

Colombelli J, Besser A, Kress H, Reynaud EG, Girard P, Caussinus E, Haselmann U, Small JV, Schwarz US, Stelzer EH. Mechanosensing in actin stress fibers revealed by a close correlation between force and protein localization. J Cell Sci. 2009; 122:1665–1679. [PubMed: 19401336]

Cox JS, Shamu CE, Walter P. Transcriptional induction of genes encoding endoplasmic reticulum resident proteins requires a transmembrane protein kinase. Cell. 1993; 73:1197–1206. [PubMed: 8513503]

Crawford AW, Michelsen JW, Beckerle MC. An interaction between zyxin and alpha-actinin. J Cell Biol. 1992; 116:1381–1393. [PubMed: 1541635]

Crocker JC, Grier DG. J Colloid Interface Sci. 1996; 179:298.

Drees B, Friederich E, Fradelizi J, Louvard D, Beckerle MC, Golsteyn RM. Characterization of the interaction between zyxin and members of the Ena/vasodilator-stimulated phosphoprotein family of proteins. J Biol Chem. 2000; 275:22503–22511. [PubMed: 10801818]

Farge E. Mechanical induction of Twist in the Drosophila foregut/stomodeal primordium. Curr Biol. 2003; 13:1365–1377. [PubMed: 12932320]

Fradelizi J, Noireaux V, Plastino J, Menichi B, Louvard D, Sykes C, Golsteyn RM, Friederich E. ActA and human zyxin harbour Arp2/3-independent actin-polymerization activity. Nat Cell Biol. 2001; 3:699–707. [PubMed: 11483954]

Gardel ML, Sabass B, Ji L, Danuser G, Schwarz US, Waterman CM. Traction stress in focal adhesions correlates biphasically with actin retrograde flow speed. J Cell Biol. 2008; 183:999–1005. [PubMed: 19075110]

Grinnell F. Fibroblast-collagen-matrix contraction: growth-factor signalling and mechanical loading. Trends Cell Biol. 2000; 10:362–365. [PubMed: 10932093]

Guo WH, Wang YL. Retrograde fluxes of focal adhesion proteins in response to cell migration and mechanical signals. Mol Biol Cell. 2007; 18:4519–4527. [PubMed: 17804814]

Harris AK, Wild P, Stopak D. Silicone rubber substrata: a new wrinkle in the study of cell locomotion. Science. 1980; 208:177–179. [PubMed: 6987736]

Heydemann A, McNally EM. Consequences of disrupting the dystrophin-sarcoglycan complex in cardiac and skeletal myopathy. Trends Cardiovasc Med. 2007; 17:55–59. [PubMed: 17292047]

Hirata H, Tatsumi H, Sokabe M. Mechanical forces facilitate actin polymerization at focal adhesions in a zyxin-dependent manner. J Cell Sci. 2008; 121:2795–2804. [PubMed: 18682496]

Hoffman LM, Jensen CC, Kloeker S, Wang CL, Yoshigi M, Beckerle MC. Genetic ablation of zyxin causes Mena/VASP mislocalization, increased motility, and deficits in actin remodeling. J Cell Biol. 2006; 172:771–782. [PubMed: 16505170]

Hutson MS, Tokutake Y, Chang MS, Bloor JW, Venakides S, Kiehart DP, Edwards GS. Forces for morphogenesis investigated with laser microsurgery and quantitative modeling. Science. 2003; 300:145–149. [PubMed: 12574496]

Iba T, Sumpio BE. Morphological response of human endothelial cells subjected to cyclic strain in vitro. Microvasc Res. 1991; 42:245–254. [PubMed: 1779881]

Iwamoto H, Nakamuta M, Tada S, Sugimoto R, Enjoji M, Nawata H. A p160ROCK-specific inhibitor, Y-27632, attenuates rat hepatic stellate cell growth. J Hepatol. 2000; 32:762–770. [PubMed: 10845663]

Ji L, Danuser G. Tracking quasi-stationary flow of weak fluorescent signals by adaptive multi-frame correlation. J Microsc. 2005; 220:150–167. [PubMed: 16363999]

Kozutsumi Y, Segal M, Normington K, Gething MJ, Sambrook J. The presence of malfolded proteins in the endoplasmic reticulum signals the induction of glucose-regulated proteins. Nature. 1988; 332:462–464. [PubMed: 3352747]

Krieg M, Arboleda-Estudillo Y, Puech PH, Kafer J, Graner F, Muller DJ, Heisenberg CP. Tensile forces govern germ-layer organization in zebrafish. Nat Cell Biol. 2008; 10:429–436. [PubMed: 18364700]

Kumar S, Maxwell IZ, Heisterkamp A, Polte TR, Lele TP, Salanga M, Mazur E, Ingber DE. Viscoelastic retraction of single living stress fibers and its impact on cell shape, cytoskeletal organization, and extracellular matrix mechanics. Biophys J. 2006; 90:3762–3773. [PubMed: 16500961]

Langanger G, Moeremans M, Daneels G, Sobieszek A, De Brabander M, De Mey J. The molecular organization of myosin in stress fibers of cultured cells. J Cell Biol. 1986; 102:200–209. [PubMed: 3510218]

Lauffenburger DA, Horwitz AF. Cell migration: a physically integrated molecular process. Cell. 1996; 84:359–369. [PubMed: 8608589]

Lazarides E, Burridge K. Alpha-actinin: immunofluorescent localization of a muscle structural protein in nonmuscle cells. Cell. 1975; 6:289–298. [PubMed: 802682]

Lee SE, Kamm RD, Mofrad MR. Force-induced activation of talin and its possible role in focal adhesion mechanotransduction. J Biomech. 2007; 40:2096–2106. [PubMed: 17544431]

Lele TP, Pendse J, Kumar S, Salanga M, Karavitis J, Ingber DE. Mechanical forces alter zyxin unbinding kinetics within focal adhesions of living cells. J Cell Physiol. 2006; 207:187–194. [PubMed: 16288479]

Lo CM, Buxton DB, Chua GC, Dembo M, Adelstein RS, Wang YL. Nonmuscle myosin IIb is involved in the guidance of fibroblast migration. Mol Biol Cell. 2004; 15:982–989. [PubMed: 14699073]

McBeath R, Pirone DM, Nelson CM, Bhadriraju K, Chen CS. Cell shape, cytoskeletal tension, and RhoA regulate stem cell lineage commitment. Dev Cell. 2004; 6:483–495. [PubMed: 15068789]

Niebuhr K, Ebel F, Frank R, Reinhard M, Domann E, Carl UD, Walter U, Gertler FB, Wehland J, Chakraborty T. A novel proline-rich motif present in ActA of Listeria monocytogenes and cytoskeletal proteins is the ligand for the EVH1 domain, a protein module present in the Ena/VASP family. EMBO J. 1997; 16:5433–5444. [PubMed: 9312002]

Nix DA, Fradelizi J, Bockholt S, Menichi B, Louvard D, Friederich E, Beckerle MC. Targeting of zyxin to sites of actin membrane interaction and to the nucleus. J Biol Chem. 2001; 276:34759–34767. [PubMed: 11395501]

Palmer BM. Thick filament proteins and performance in human heart failure. Heart Fail Rev. 2005; 10:187–197. [PubMed: 16416042]

Paszek MJ, Weaver VM. The tension mounts: mechanics meets morphogenesis and malignancy. J Mammary Gland Biol Neoplasia. 2004; 9:325–342. [PubMed: 15838603]

Peterson LJ, Rajfur Z, Maddox AS, Freel CD, Chen Y, Edlund M, Otey C, Burridge K. Simultaneous stretching and contraction of stress fibers in vivo. Mol Biol Cell. 2004; 15:3497–3508. [PubMed: 15133124]

Peyton SR, Raub CB, Keschrumrus VP, Putnam AJ. The use of poly(ethylene glycol) hydrogels to investigate the impact of ECM chemistry and mechanics on smooth muscle cells. Biomaterials. 2006; 27:4881–4893. [PubMed: 16762407]

Reinhard M, Zumbrunn J, Jaquemar D, Kuhn M, Walter U, Trueb B. An alpha-actinin binding site of zyxin is essential for subcellular zyxin localization and alpha-actinin recruitment. J Biol Chem. 1999; 274:13410–13418. [PubMed: 10224105]

Sabass B, Gardel ML, Waterman CM, Schwarz US. High resolution traction force microscopy based on experimental and computational advances. Biophys J. 2008; 94:207–220. [PubMed: 17827246]

Sadoshima J, Izumo S. The cellular and molecular response of cardiac myocytes to mechanical stress. Annu Rev Physiol. 1997; 59:551–571. [PubMed: 9074777]

Sawada Y, Tamada M, Dubin-Thaler BJ, Cherniavskaya O, Sakai R, Tanaka S, Sheetz MP. Force sensing by mechanical extension of the Src family kinase substrate p130Cas. Cell. 2006; 127:1015–1026. [PubMed: 17129785]

Shaner NC, Campbell RE, Steinbach PA, Giepmans BN, Palmer AE, Tsien RY. Improved monomeric red, orange and yellow fluorescent proteins derived from Discosoma sp. red fluorescent protein. Nat Biotechnol. 2004; 22:1567–1572. [PubMed: 15558047]

Tamada M, Sheetz MP, Sawada Y. Activation of a signaling cascade by cytoskeleton stretch. Dev Cell. 2004; 7:709–718. [PubMed: 15525532]

Wang N, Butler JP, Ingber DE. Mechanotransduction across the cell surface and through the cytoskeleton. Science. 1993; 260:1124–1127. [PubMed: 7684161]

Wang Y, Botvinick EL, Zhao Y, Berns MW, Usami S, Tsien RY, Chien S. Visualizing the mechanical activation of Src. Nature. 2005; 434:1040–1045. [PubMed: 15846350]

Wozniak MA, Chen CS. Mechanotransduction in development: a growing role for contractility. Nat Rev Mol Cell Biol. 2009; 10:34–43. [PubMed: 19197330]

Yoshigi M, Hoffman LM, Jensen CC, Yost HJ, Beckerle MC. Mechanical force mobilizes zyxin from focal adhesions to actin filaments and regulates cytoskeletal reinforcement. J Cell Biol. 2005; 171:209–215. [PubMed: 16247023]

Zamir E, Geiger B. Molecular complexity and dynamics of cell-matrix adhesions. J Cell Sci. 2001; 114:3583–3590. [PubMed: 11707510]

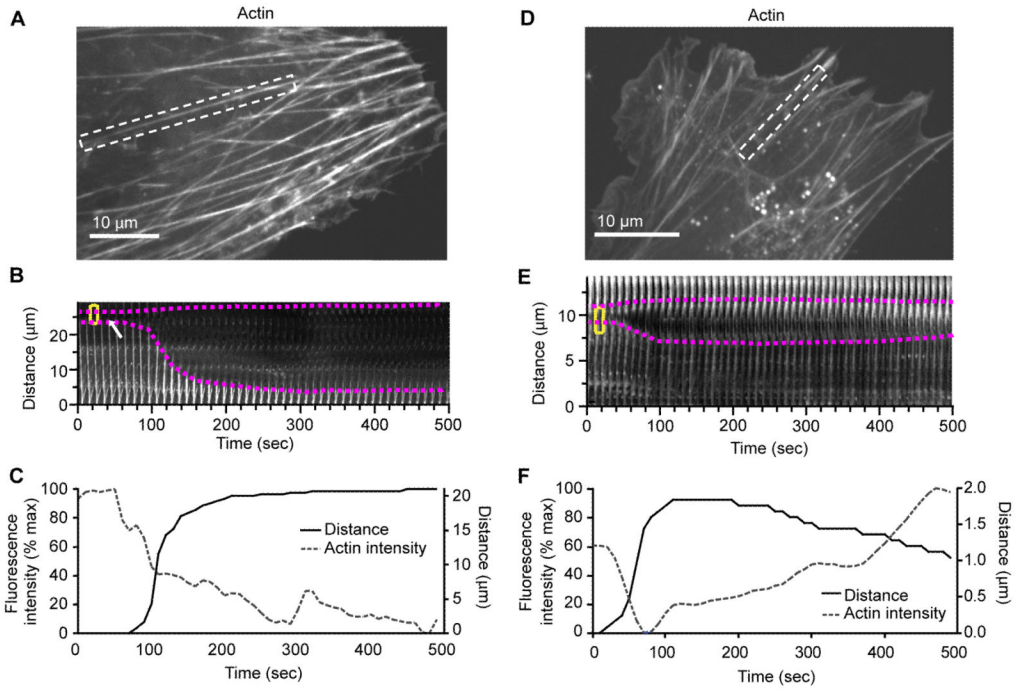

Figure 1.

SFs display the capacity to repair local damage.

The micrographs and kymographs are of actin-mCherry in mouse fibroblasts.

For this and subsequent figures, plots below kymographs show normalized average fluorescence intensity in the dotted yellow box over time and distance change between the fiducials highlighted with magenta dots.

(See Movie S1)

(A) Stress fiber in dashed white box undergoes catastrophic break.

(B) Kymograph showing SF highlighted in (A) that thins, breaks, and recoils. White arrow shows region of SF thinning prior to the break.

(C) Intensity and distance plot of (B) catastrophic SF break. Lack of rise in actin fluorescence intensity after ~100s indicates a catastrophic break.

(D) Stress fiber in dashed white box undergoes strain followed by repair.

(E) Kymograph showing SF highlighted in (D) undergoes thinning, elongation, and then repair.

(F) Intensity and distance graph of SF thinning, elongation and repair. Rise in actin fluorescence intensity after ~100s indicates SF repair.

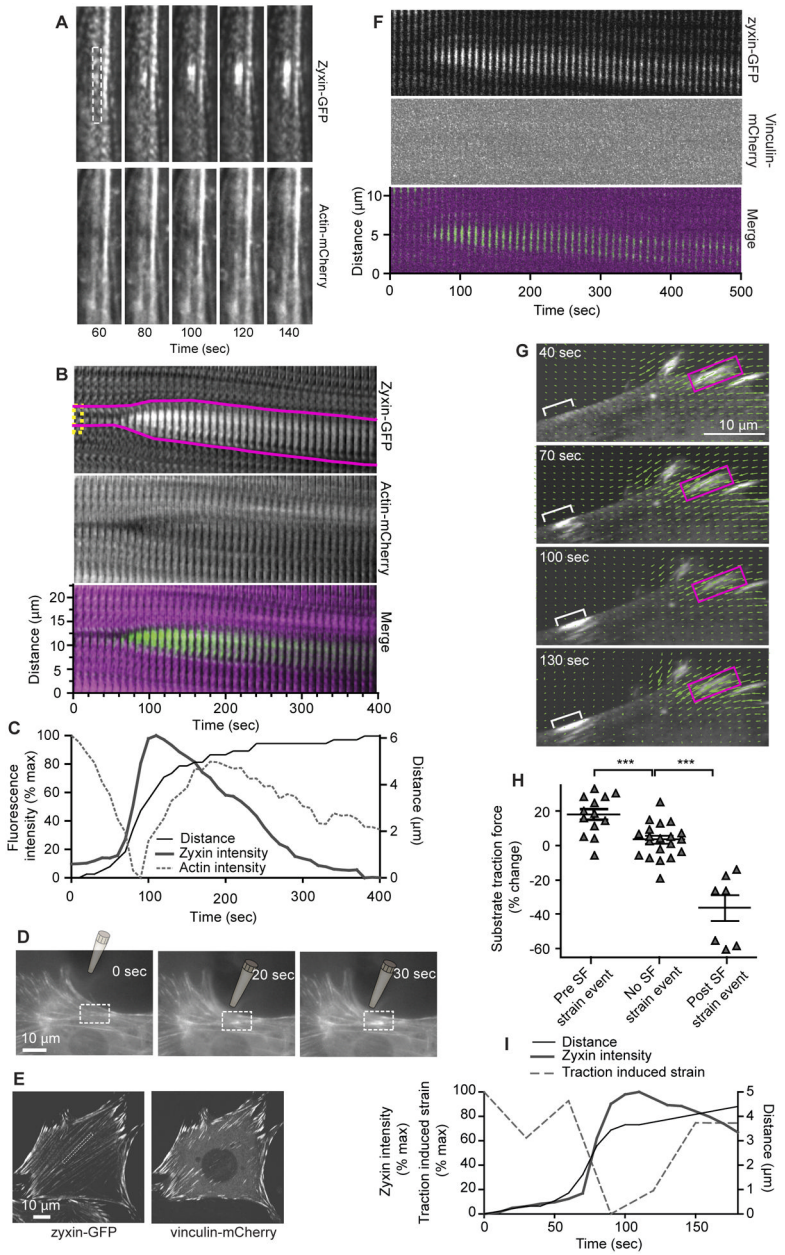

Figure 2.

Zyxin is recruited to sites of SF strain.

(A) Time-lapse series of zyxin-GFP, and actin-mCherry shows zyxin accumulation at a site of SF damage. (See Movie S2 and Movie S3 as an additional example)

(B) Kymograph from the dashed white box in (A) showing rapid zyxin accumulation at a region of SF strain. For merge, zyxin is green, actin is magenta.

(C) Plot from (B) of intensity over time and distance change between the fiducials highlighted with magenta lines.

(D) Images of zyxin-GFP expressing cell prodded by a micropipette. Zyxin-GFP accumulates at the site of SF inflection (white box)(see Movie S4).

(E) Micrographs showing zyxin-GFP and vinculin-mCherry expression.

(F) Kymograph made from the dashed white box in (E) showing no vinculin accumulation at the site of zyxin accumulation.
(G) Traction microscopy of zyxin-GFP expressing cell. Green vectors show the interpolated traction-induced strain map of bead positions relative to their cell-free positions (see Movie S5). Bracket highlights the local accumulation of zyxin-GFP on the SF that terminates at the FA outlined by the magenta box.
(H) When compared to quiescent SFs (n=20), SF strain events are preceded by a net increase in traction force (n=13), and are followed by a net decline in traction force (n=7). Error bars show SEM.
(I) Normalized traction-induced strain integrated within the region containing the FA (magenta boxes in (E)).When the attached SF elongates (plotted as distance) and zyxin accumulates (normalized fluorescence intensity in the bracketed region in (E)) there is an acute drop in traction-induced strain at the FA.

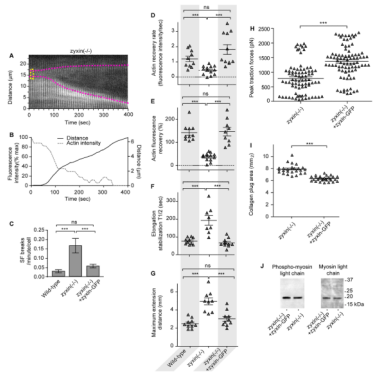

Figure 3.

Stress fiber strain sites fail to stabilize in zyxin (−/ −) cells.

(A) Kymograph of actin-mCherry expressed in a zyxin (−/ −) cell showing a SF strain event that fails to recover (See Movie S6).

(B) Plot from (A) of intensity over time and distance change between the fiducials highlighted with magenta dots. Lack of rise in actin fluorescence intensity and increasing distance between fiducials after ~100s indicates lack of SF repair.

(C) Catastrophic SF break frequency in wild-type (n=83 cells), zyxin (−/ −) (n= 57 cells) and zyxin (−/ −) + zyxin-GFP (n= 172 cells).

(D) Wild-type (n=10) and rescued (n=13) cells show enhanced rate of actin recovery at SF strain sites when compared to zyxin (−/ −) cells (n=13) (p=0.0002).

(E) Wild-type (n=10 events) and rescued (n=13 events) cells show enhanced net actin recovery at SF strain sites when compared to zyxin (−/ −) cells (n=13 events) (p<0.0001).

(F) Wild-type (n=10 events) and rescued (n=10 events) cells show decreased half-time to the stabilization at SF strain sites when compared to zyxin (−/ −) cells (n= 8 events) (p=0.0002).

(G) Wild-type (n=10 events) and rescued (n=10 events) cells show decreased maximum elongation at SF strain sites when compared to zyxin (−/ −) cells (n=9 events) (p=0.0006).

(H) Zyxin (−/ −) cells (n=80) showed decreased peak traction forces when compared to zyxin (−/ −)+zyxin-GFP cells (n=89) (P<0.0001)(see also Figure S2).

(I) Zyxin (−/ −) cells (n=25) showed decreased collagen plug contraction when compared to zyxin (−/ −) cells +zyxin-GFP (n=28) (P<0.0001).

(J) Western blot analysis showing unchanged myosin light chain ser19 phosphorylation levels in zyxin (−/ −) and zyxin (−/ −)+ zyxin-GFP cells (n=3). Plots (D–I) show Mean +/− SEM

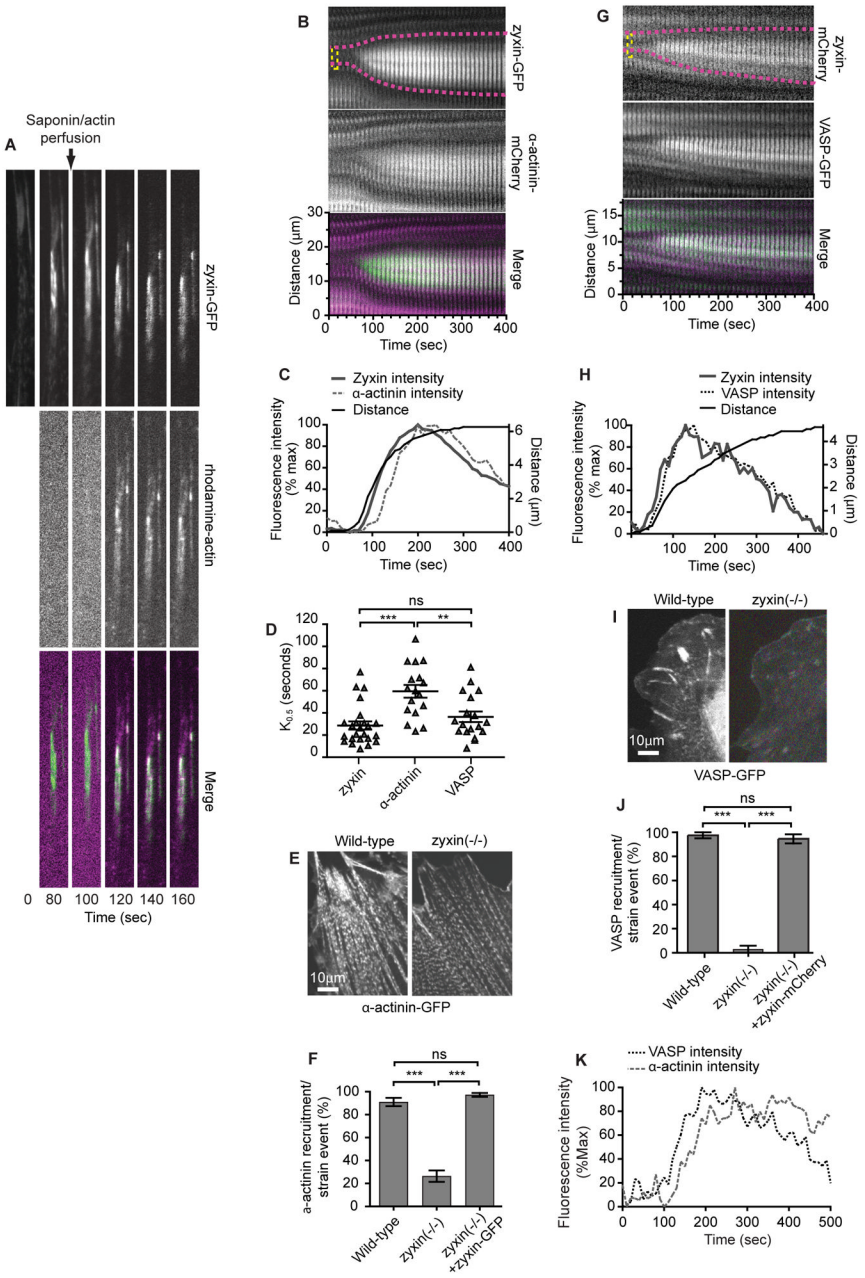

Figure 4.

Stress fiber strain sites generate free actin barbed ends and accumulate α-Actinin and VASP in a zyxin-dependent manner.

(A) Image sequence showing rhodamine–actin accumulation at SF strain sites (See Movie S7).

(B) Kymograph of zyxin-GFP and α-actinin-mCherry expressed in zyxin (−/ −) cell. For merge, zyxin is green, α-actinin is magenta.

(C) Intensity and distance graph showing α-actinin accumulates at SF strain sites lagging zyxin accumulation (see Movie S8).

(D) Half-time of protein accumulation at SF strain sites shows α-actinin (n=17) accumulation lags both zyxin (n=24)(p=0.0043) and VASP (n=18)(p=0.0133)(see also Figure S3).
(E) α-Actinin-GFP periodic distribution pattern on SF persists in zyxin (−/ −) cells.
(F) Zyxin (−/ −) cells (n=421) cells show a decreased percentage of α-actinin recruitment to SF strain sites when compared to wild-type (n=233) and rescued (n=364) cells (see Movie S8).
(G) Kymograph of VASP-GFP and zyxin-mCherry expressed in zyxin (−/ −) cell. For merge, VASP is green, zyxin is magenta.
(H) Intensity and distance graph showing VASP accumulates at SF strain sites coincident with zyxin (see Movie S9).
(I) VASP fails to localize on SFs in zyxin (−/ −) cells.
(J) Zyxin (−/ −) cells (n=31) show decreased percentage of VASP recruitment to SF strain sites when compared to wild-type (n=99) and rescued (n=171) cells (see Movie S9).
(K) Intensity plot showing α-actinin accumulation lags VASP in a dual labeled cell. Data are shown as mean+/− SEM

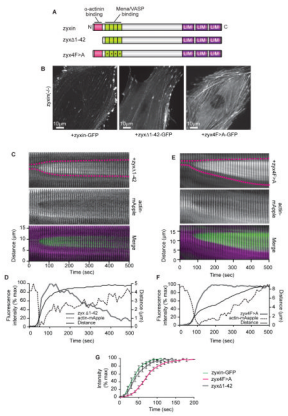

Figure 5.

Zyxin accumulation at SF strain sites is not dependent on zyxin's interaction with α-actinin, but is facilitated by interaction with VASP.

(A) Schematic of wild-type zyxin and zyxin mutated to interfere with α-actinin binding (zyxΔ1-42), or Mena/VASP protein binding (zyx4F>A).

(B) Mutant zyxin zyxΔ1-42 and zyx4F>A localize to SFs in zyxin (−/ −) cells.

(C) Kymograph of zyxΔ1-42 and actin-mApple expressed in zyxin (−/ −) cell. For merge, zyx 1-42 is green, actin is magenta.

(D) Intensity and distance graph showing zyxΔ1-42 accumulates at SF strain sites.

(E) Kymograph of zyx4F>A and actin-mApple expressed in zyxin (−/ −) cell. For merge, zyx4F>A is green, actin is magenta.

(F) Intensity and distance graph showing zyx4F>A accumulates at SF strain sites.

(G) Zyx4F>A (n=12) accumulation at stress fiber strain sites is slower than wild-type zyxin (n=13) ($p<0.0001$) or zyxΔ1-42 (n=12) ($p=0.0002$).

Data are shown as mean+/− SEM

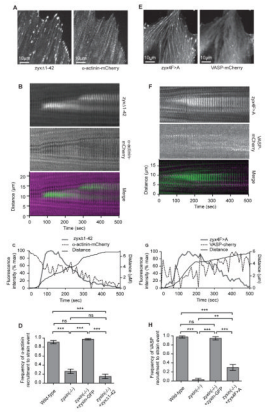

Figure 6.

α-Actinin and VASP fail to accumulate at SF strain sites in zyxin (−/ −) cells reconstituted with zyxΔ1-42 or zyx4F>A, respectively.

(A) α-actinin localizes on SFs in zyxin (−/ −) cells expressing zyxΔ1-42 transgene.

(B) Kymograph of zyxΔ1-42 and α-actinin-mCherry expressed in zyxin (−/ −) cell. For merge, zyxΔ1-42is green, α-actinin is magenta.

(C) Intensity and distance plot showing loss of robust α-actinin accumulation at stress fiber strain site in zyxin (−/ −) cell expressing zyxΔ1-42.

(D) Percent SF strain events that recruit α-actinin in wild-type (n= 233), zyxin (−/ −) (n= 421), zyxin (−/ −) + zyxin-GFP (n=364) and zyxin (−/ −) + zyxΔ1-42 (n=47) cells.

(E) VASP fails to localize on SFs and FAs in zyxin (−/ −) cells expressing zyx4F>A.

(F) Kymograph of zyx4F>A and VASP-mCherry expressed in zyxin (−/ −) cell. For merge, zyx4F>A is green, VASP is magenta.

(G) Intensity and distance graph showing loss of VASP accumulation at stress fiber strain site in zyxin (−/ −) cell expressing zyx4F>A.

(H) Percent SF strain events that recruit VASP in wild-type (n= 99), zyxin (−/ −) (n= 31), zyxin (−/ −) +zyxin-GFP (n=171) and zyxin (−/ −) +zyx4F>A (n=38) cells. Data are shown as mean+/− SEM

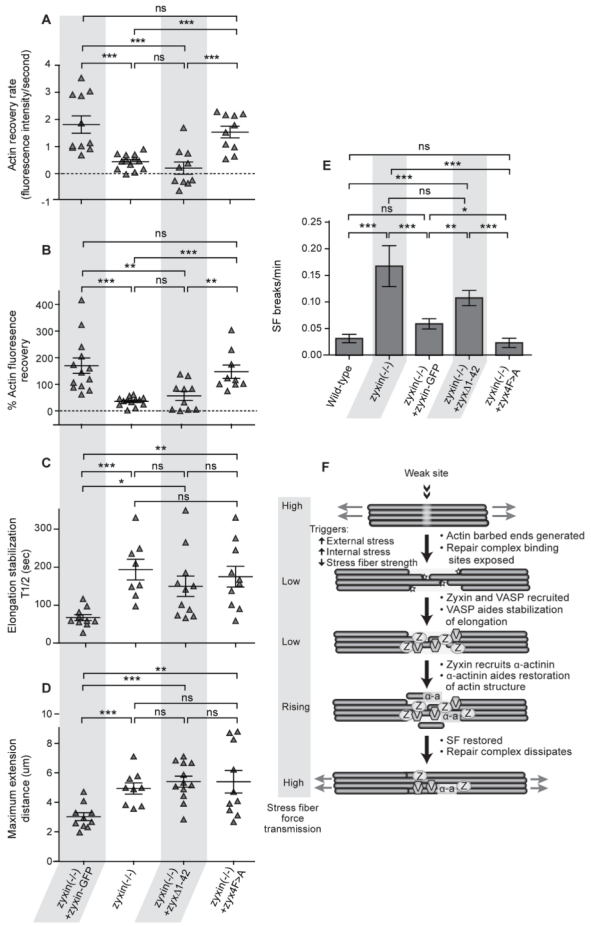

Figure 7.

Zyxin rescue constructs mutated to eliminate α-actinin or VASP binding fail to rescue SF strain phenotypes seen in zyxin (−/ −) cells.

(A) Recovery rate of actin intensity immediately following thinning in zyxin (−/ −) +zyxin-GFP (n=13), zyxin (−/ −) (n= 13), zyxin (−/ −) +zyxΔ1-42 (n= 10) and zyxin (−/ −) +zyx4F>A (n= 10) cells.

(B) Percent recovery of actin signal post-thinning event in zyxin (−/ −) +zyxin-GFP (n= 13), zyxin (−/ −) (n= 13), zyxin (−/ −) +zyxΔ1-42 (n= 10) and zyxin (−/ −) +zyx4F>A (n= 9) cells.

(C) Half-time to stabilization of fiber elongation during a strain event in zyxin (−/ −) +zyxin-GFP (n= 10), zyxin (−/ −) (n= 8), zyxin (−/ −) +zyxΔ1-42 (n=11) and zyxin (−/ −) +zyx4F>A (n= 10) cells.

(D) Maximum elongation of the stress fiber region undergoing a strain event in zyxin (−/ −) +zyxin-GFP (n=10), zyxin (−/ −) (n= 9), zyxin (−/ −) +zyxΔ1-42 (n= 12) and zyxin (−/ −) +zyx4F>A (n= 10) cells.

(E) Catastrophic stress fiber break frequency in wild-type (n=83), zyxin (−/ −) (n= 57), zyxin (−/ −) +zyxin-GFP (n= 172), zyxin (−/ −) +zyxΔ1-42 (n= 140) and zyxin (−/ −) +zyx4F>A (n= 103) cells.

(F) Model for recruitment of a zyxin mediated repair complex to sites of SF strain.

Data are shown as mean+/− SEM